this refinement are listed in Tables III and IV,[13] respectively. A final difference synthesis revealed that the largest residual electron density of 0.49 e/Å^3 was in the region close to a disordered ethyl carbon.

The asymmetric unit of structure contains a discrete anion of $[(\eta^5\text{-}C_5H_5)Ni(C_6F_5)_2]^-$ and half of two $[(C_2H_5)_4N]^+$ cations that reside on crystallographically independent centers of inversion with disordered methylene carbon atoms. The anion, depicted in Figure 1,[8] consists of a nickel atom that is σ-bonded to two C_6F_5 ligands and π-bonded to C_5H_5 in η^5 fashion. This arrangement has quasi $m(C_s)$ symmetry with the quasi mirror plane containing the Ni, C_1, C_7, and C_{13} atoms and bisecting the C_{15}–C_{16} bond. The plane of the C_5H_5 ring is within 1° of being perpendicular to the Ni, C_1, C_7 plane and the C_1NiC_7 bond angle is 92.7 (1)°. The average Ni–C_6F_5 bond distance of 1.900 (3) Å is 0.009 Å longer than the corresponding distance in $(\eta^6\text{-}C_6H_5CH_3)Ni(C_6F_5)_2$.[1c] Bond distances and angles are compiled in Tables V[13] and VI,[13] respectively. Other bond parameters within the planar C_6F_5 ligands are within experimental error equivalent to those in $(\eta^6\text{-}C_6H_5CH_3)Ni(C_6F_5)_2$.[1c]

The average Ni–C_{Cp} distance is 2.108 (4) Å; the five distances are not equivalent due to a nonplanar deformation of the η^5-C_5H_5 ring. This deformation can be described as a displacement of C_{13} from the plane containing C_{14}, C_{15}, C_{16}, and C_{17} by 0.070 (5) Å toward the Ni atom, resulting in a fold angle (about the line between C_{14} and C_{17}) of 5.5°. Alternatively, if the plane defined by C_{13}, C_{15}, and C_{16} is taken as the reference plane, then C_{14} and C_{17} are 0.049 (4) and 0.040 (5) Å, respectively, out of the plane away from the Ni atom.[7] The results of mean-planes calculations are given in Table VII.[13] This second description is comparable to that used to describe the nonplanar deformation in $(\eta^6\text{-}C_6H_5CH_3)Ni(C_6F_5)_2$,[1c] which can be explained by electronic factors.[9] Interestingly, a similar deformation has been observed in $(\eta^5\text{-}C_5H_5)Ni(GeCl_3)(PPh_3)$,[10] while the C_5H_5 ring in $(\eta^5\text{-}C_5H_5)Ni(C_6F_5)(PPh_3)$[11] is planar.

The product $[(\eta^5\text{-}Cp)Ni(C_6F_5)_2][Et_4N]$, which is isoelectronic with the starting arene complex, represents a new class of cyclopentadienylnickel(II) organometallics. No $[(\eta^5\text{-}Cp)Ni(R)_2]^-$ complexes have been reported. Actually $(\eta^5\text{-}Cp)Ni$ anions are rare, the most notable being $[CpNi(CO)]^-$, which is unstable and is generally trapped at low temperature by nucleophilic displacement of halide from various RX compounds.[12]

A typical preparative reaction is now described. All manipulations were carried out under a nitrogen atmosphere in dry, deoxygenated solvents. When a toluene solution (30 mL) of $(\eta^6\text{-toluene})Ni(C_6F_5)_2$ (0.5 g, 1 mmol) held at −78 °C was treated with 1 equiv of solid TlCp (0.275 g, 1 mmol) followed by warming, the mixture became homogeneous between −10 and 0 °C with a color change from red-brown to green. The mixture was stirred for 3 h at room temperature. Recooling to −78 °C and addition of a 4-fold excess of Et_4NI crystals followed again by slow warming to room temperature resulted in a light green supernate and a green solid. The supernate was removed and discarded. The solid was washed twice with 10-mL portions of toluene and twice with 20-mL portions of Et_2O and was then extracted with THF and filtered. After concentration of the ethereal solution, analytically pure product was obtained by vapor diffusion of pentane into the THF solution. Alternatively, evaporation of the THF, dissolution in a 15:85 (v/v) mixture of CH_2Cl_2/Et_2O followed by cooling also produced the pure salt. The product $[CpNi(C_6F_5)_2][Et_4N]$ is a yellow-green air-stable solid, soluble in CH_2Cl_2, THF, CH_3CN, and acetone, slightly soluble in Et_2O, and insoluble in petroleum ether and water. The complex is decomposed by $CHCl_3$. Yields were 60–80%. Mp: 149.5 °C (uncor).

^{1}H NMR (400 MHz, acetone-d_6, Me_4Si reference): δ(Cp) 5.16 (S, 5 H), (CH_2) 3.51 (q, 8 H, $^3J_{HH}$ = 7.0 Hz), $\delta(CH_3)$ 1.4 (tt, 12 H, $^3J_{NH}$ = 1.5 Hz, $^3J_{HH}$ = 7 Hz). $^{13}C\{^1H\}$ NMR (acetone-d_6): δ(Cp) 89.6, $\delta(CH_2)$ 53.1, $\delta(CH_3)$ 7.7. IR (cm^{-1}, KBr pellet): 3050 w, 1690 vw, 1615 vw, 1500 vs, 1455 vs, 1360 m, 1280 w, 1180 m, 1055 vs, 1010 m, 960 vs, 860 w, 690 vs. Anal. Calcd: C, 51.0; H, 4.31; N, 2.35. Found: C, 51.5; H, 4.30; N, 2.58.

Registry No. $[(\eta^5\text{-}C_5H_5)Ni(C_6F_5)_2]^-[(C_2H_5)_4N]^+$, 97645-18-6; $(\eta^6\text{-}C_6H_5CH_3)Ni(C_6F_5)_2$, 66197-14-6; TlCp, 34822-90-7.

Supplementary Material Available: Listings of structure factor amplitudes (Table II), anisotropic thermal parameters (Table IV), bond distances (Table V), bond angles (Table VI), and mean-planes calculations (Table VII) (30 pages). Ordering information is given on any current masthead page.

(7) J. J. Park's block-diagonal-refinement program REFINE was used. Because block-diagonal refinement was used, estimated standard deviations were calculated by using only correlations between coordinates and are underestimated.

(8) Johnson, D. K. "ORTEP, a Fortran Thermal Ellipsoid Plot Program for Crystal Structure Illustration", Report ORNL-3974, Oak Ridge National Laboratory: Oak Ridge, TN, 1965.
(9) Radonovich, L. J.; Koch, F. J.; Albright, T. A. *Inorg. Chem.* **1980**, *19*, 3373.
(10) Bell, N. A.; Glocking, F.; McGregor, A.; Schneider, M. L.; Schearer, H. M. M. *Acta Crystallogr., Sect. C: Cryst. Struct. Commun.* **1984**, *C40*, 623–625.
(11) Churchill, M. R.; O'Brien, T. A. *J. Chem. Soc. A* **1968**, 2970–2976.
(12) Jolly, J. W. In "Comprehensive Organometallic Chemistry", Wilkinson, G., Stone, F. G. A., Abel, E. W., Eds.; Pergamon Press: New York, 1983; Vol. 6, Chapter 37.8, pp 189–228.
(13) Supplementary material.

Contribution from the Departments of Chemistry, Universität Zürich, CH-8057 Zürich, Switzerland, Philipps-Universität, D-3550 Marburg, Germany, and Kansas State University, Manhattan, Kansas 66506

Metal π Complexes of Benzene Derivatives. 22.[1] Ground-State Configuration of $(\eta^6$-Toluene)bis$(\eta^1$-pentafluorophenyl)cobalt(II): An EPR Study

John H. Ammeter,[2a] Christoph Elschenbroich,*[2b] Thomas J. Groshens,[2c] Kenneth J. Klabunde,[2c] R. Oskar Kühne,[2a] and Reinhart Möckel[2b]

Received September 19, 1983

The observation[3] that bis(pentafluorophenyl)cobalt(II) produced via cocondensation of cobalt atoms with pentafluorobromobenzene vapor adds a toluene molecule to yield the novel paramagnetic $(\eta^6$-toluene)bis(pentafluorophenyl)cobalt(II) inaugurated the field of $(\eta$-arene)ML_2 chemistry, which continues to reveal many interesting aspects structurally[4,5] as well as chemically.[6] One outstanding feature of this new class of π complexes is the facile substitution of η^6-toluene for other arenes. This has been attributed to the weakness of the transition-metal–arene bond and rationalized in terms of the occupation of an antibonding orbital by one or two electrons (M = Co, Ni, respectively).[5] The availability of the isostructural[4] complexes $(\eta^6\text{-tol})Co(\eta^1\text{-}C_6F_5)_2$ and $(\eta^6\text{-tol})Ni(\eta^1\text{-}C_6F_5)_2$ prompted us to engage in a thorough powder and single-crystal EPR investigation, the results of which are reported in the present communication. The principal aim was the identification of the singly occupied MO in complexes of the general formula (arene)ML_2, with $(\eta^6\text{-tol})Co(\eta^1\text{-}C_6F_5)_2$ serving as a representative example.

(1) Part 21: Elschenbroich, Ch.; Möckel, R. *Z. Naturforsch., B: Anorg. Chem., Org. Chem.* **1984**, *39B*, 375.
(2) (a) Universität Zürich. (b) Universität Marburg. (c) Kansas State University.
(3) Anderson, B. B.; Behrens, C. L.; Radonovich, L. J.; Klabunde, K. J. *J. Am. Chem. Soc.* **1976**, *98*, 5390.
(4) Radonovich, L. J.; Klabunde, K. J.; Behrens, C. B.; McCollor, D. P.; Anderson, B. B. *Inorg. Chem.* **1980**, *19*, 1221.
(5) Radonovich, L. J.; Koch, F. J.; Albright, Th. *Inorg. Chem.* **1980**, *19*, 3373.
(6) (a) Klabunde, K. J.; Anderson, B. B.; Bader, M.; Radonovich, L. J. *J. Am. Chem. Soc.* **1978**, *100*, 1313. (b) Brezinski, M. M.; Klabunde, K. J. *Organometallics* **1983**, *2*, 1116.

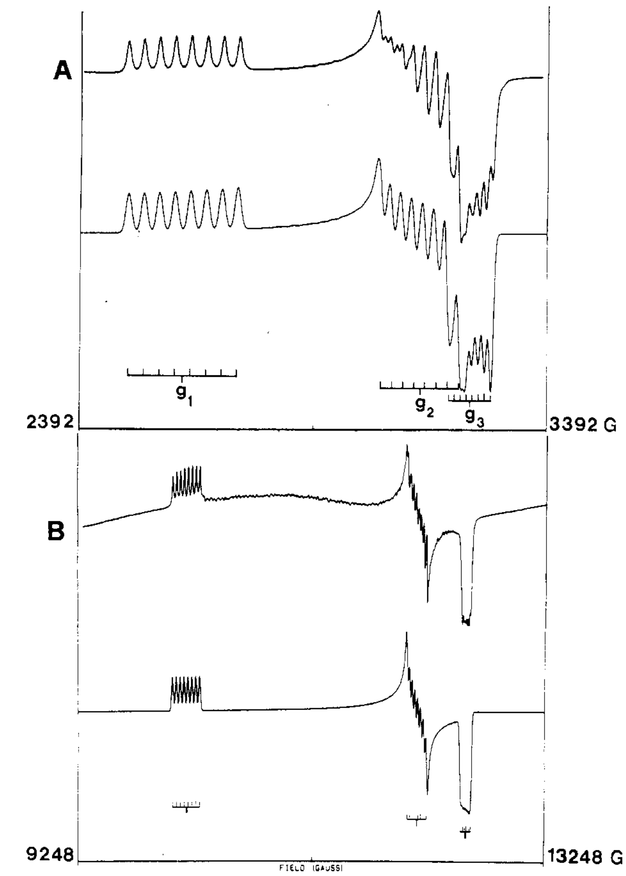

Figure 1. EPR spectra of polycrystalline (tol)$Co(C_6F_5)_2$ (2%) in (tol)$Ni(C_6F_5)_2$: (a) X-band (8.987 GHz), T = 4 K, scan range = 1000 G; (B) Q-band (35.005 GHz), T = 103 K, scan range = 4000 G. Lower traces are computed simulations[21,22] with the following linewidth tensors (G): (A) W_x = 13, W_y = 13, W_z = 10; (B) W_x = 16, W_y = 16, W_z = 14. A Gaussian lineshape was assumed in the simulations.

Experimental Section

The complexes (η^6-tol)Co(η^1-$C_6F_5)_2$ and (η^6-tol)Ni(η^1-$C_6F_5)_2$ were prepared as reported previously.[3] Magnetically diluted samples were obtained via crystallization from toluene. EPR measurements were carried out on fluid solutions of the cobalt complex (10^{-3} M in toluene-d_8 and pentane, respectively), on rigid solutions (toluene-d_8), on powders of the cobalt complexes diluted in the analogous nickel complex (1:50), and on a single crystal (1:50). The spectra were recorded on an E 12 EPR spectrometer (Varian) equipped with a Varian E-500 NMR gaussmeter and an EIP Model 548 microwave frequency counter in the X- as well as the Q-band. Sample preparation has to be performed under exclusion of air and moisture.

Results and Discussion

In fluid solution, only a single broad signal void of hyperfine structure is observed for (tol)$Co(C_6F_5)_2$. This is in accord with the considerable g and ^{59}Co hyperfine anisotropy that emerges from the spectra recorded in rigid solution as well as in magnetically diluted polycrystalline powders. The powder spectra of randomly oriented radicals in the X- and Q-band ranges are depicted in Figure 1; the pertinent EPR parameters are listed in Table I.[7a]

Due to the more homogeneous microscopic environment in the doped polycrsytalline sample, as compared to the frozen solution, resolution in the former matrix is superior to the latter. The analysis of the spectra of randomly oriented radicals yields the six parameters $g_{1,2,3}$ and $A_{1,2,3}(^{59}Co)$.[7b] In order to use these data

(7) (a) The X-band spectra measured at 4 K and at 103 K are practically identical, whereas at room temperature only a broad asymmetric line is observed. (b) From our analysis of the powder spectra it was not possible to derive conclusive information about the relative orientation of the principal axes of **g** and **A**. In spite of the fact that the site symmetry at the cobalt position is only C_2,[4] we assumed a common principal axis system for these tensors.

Table I. EPR Parameters for (η^6-Toluene)bis(η^1-pentafluorophenyl)cobalt(II)

	X-band[a]		X- and Q-band[a]
	rigid soln[b]	single cryst[c]	polycryst powder[c]
g_x	2.459	2.457	2.458
g_y	2.059	(2.083)[d]	2.058
g_z	1.991	(1.973)[d]	1.989
$\langle g \rangle$	2.165[e]		
$A_x(^{59}Co)$, cm^{-1}	0.004 13	0.003 77	0.003 82
$A_y(^{59}Co)$, cm^{-1}	0.002 19	(0.002 18)[d]	0.002 28
$A_z(^{59}Co)$, cm^{-1}	0.001 26	(0.001 58)[d]	0.001 20

[a] T = 103 K. [b] Solvent: toluene-d_8. [c] Doped into (tol)$Ni(C_6F_5)_2$, 2%. [d] Deviations of these values from the g and A data extracted from polycrystalline powder spectra stem from difficulties in accurate alignment in the directions $\vec{H}\|\vec{a}$ and $\vec{H}\|\vec{c}$ caused by inferior development of the respective crystal faces. Whereas the values in brackets serve for the assignments $g_2 = g_y$ and $g_3 = g_z$, the accurate g and A parameters for (tol)$Co(C_6F_5)_2$ are listed in column three. [e] Fluid solution, toluene-d_8, T = 303 K, hyperfine splitting unresolved.

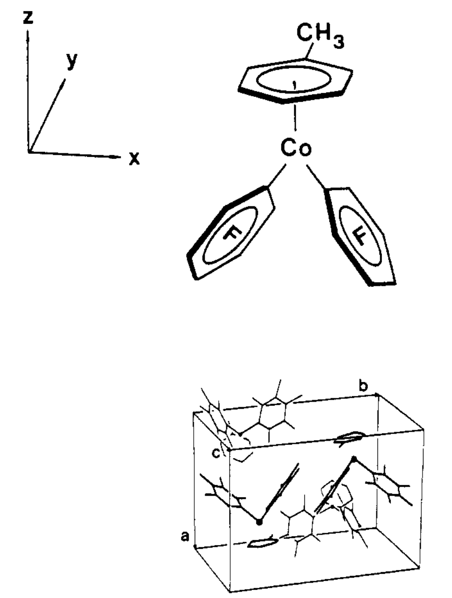

Figure 2. Molecular axis system and unit cell diagram of (tol)$M(C_6F_5)_2$, M = Co, Ni (reproduced with permission from ref 4).

to derive the electronic configuration of the paramagnetic complex, the experimental g and A values have to be related to a molecule-fixed coordinate system by purely experimental means. Toward that goal, a single crystal of (η^6-tol)Co(η^1-$C_6F_5)_2$ diluted (1:50) in its isostructural[4] Ni analogue at various orientations was studied by EPR. The unit cell of (η^6-tol)Ni(η^1-$C_6F_5)_2$ (Figure 2) contains four molecules which are pairwise related by the symmetry operation of inversion. Consequently, two magnetically inequivalent sites arise, and the single-crystal EPR spectra in general display two ^{59}Co octets centered at different g values (Figure 3). The strong overlap of the spectra stemming from the different sites would make an application of the standard procedure[8] for the extraction of **g** and **A** tensors from single-crystal spectra quite tedious because for each orientation of the specimen relative to the magnetic field the accurate g and A data required for the construction of the nondiagonal tensors would have to be obtained via optimized computer simulations of the spectral traces. However, closer inspection of the unit cell diagram (Figure 2) and the atomic coordinates[4] in conjunction with the space group *Pnma* reveals that a set of crystal orientations exists, for which both magnetically inequivalent sites have a common principal axis. This situation arises whenever the magnetic field is perpendicular to the *ac* plane of the unit cell, the field direction then being parallel to the x coordinate of the molecules. In these orientations,

(8) Schonland, D. S. *Proc. Phys. Soc., London* **1959**, *73*, 788.

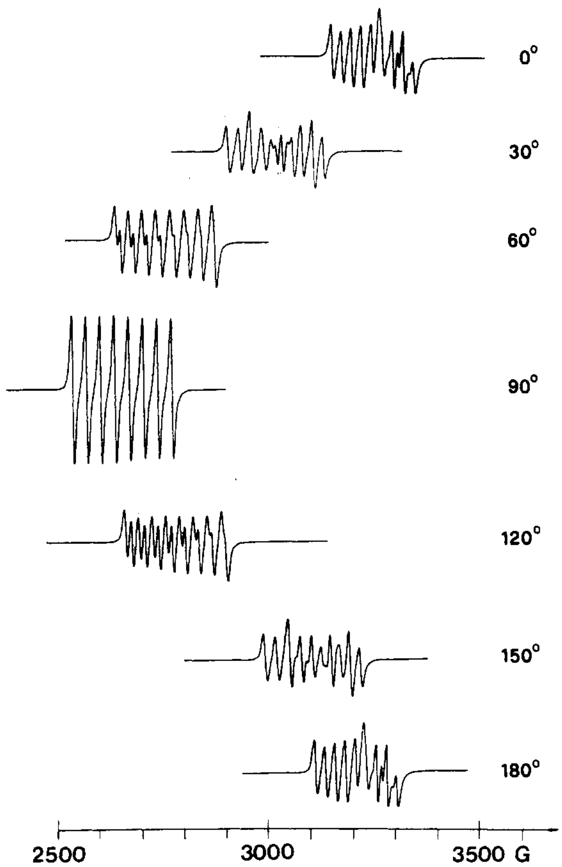

Figure 3. Single-crystal EPR spectra of (tol)Co(C_6F_5)$_2$ (2%) in (tol)-Ni(C_6F_5)$_2$ at 103 K. The spectrum at the angle designated 90° represents the orientation when the magnetic field direction is perpendicular to the largest face of the platelet-shaped crystal (*ac* plane). The behavior of the spectrum upon rotation about an axis contained in this plane is also depicted.

only *one* ^{59}Co octet should be observed. Conversely, if experimentally an orientation of the crystal can be found in which the two ^{59}Co octets have merged into one such multiplet, which is unaffected by rotation about the axis parallel to the direction of the magnetic field and which possesses a *g* factor identical with one of the *g* factors extracted from the spectra of polycrystalline material, the respective *g* and $A(^{59}\text{Co})$ values may unequivocally be assigned to the molecular *x* direction. Therefore, a doped crystal (1:50) shaped as a tetragonal platelet was mounted in three orthogonal orientations on a goniometer rod and turned in the magnetic field. The rotational behavior of the EPR absorption for one of these operations is shown in Figure 3. Whenever the field direction was perpendicular to the largest of the crystal faces (orientation 90° in Figure 3) a single ^{59}Co octet was observed. This leads to the assignment $g_x = 2.458$ and $A_x(^{59}\text{Co}) = 38.2 \times 10^{-4}$ cm^{-1}. It is gratifying to note that these values agree well with the magnitudes of g_1 and $A_1(^{59}\text{Co})$ extracted from the spectra of polycrystalline samples. As a corollary, the observation of a single (^{59}Co) octet for certain crystal orientations, considering the relative disposition of the inequivalent sites in the unit cell, implies that the molecular *x* axis and the *x* axis of the **g** tensor are collinear. The assignment of the remaining parameters $g_{2,3}$ and $A_{2,3}(^{59}\text{Co})$ to the molecular *y* and *z* coordinates required information about the orientation of the unit cell relative to the external crystal faces. This was obtained by indexing via diffractometry the crystal employed in the EPR measurement. If the crystal was positioned in the magnetic field with $\vec{a}\|\vec{H}$, again only one (^{59}Co) octet was observed since the magnetic field direction then bisects the angle between the *y* axes and the *z* axes, respectively, of the two inequivalent sites. The same is true for $\vec{c}\|\vec{H}$. In the case of $\vec{H}\|\vec{a}$, the angles $\angle\vec{H}\vec{y} = 57.5°$ and $\angle\vec{H}\vec{z} = 32.5°$ occur whereas for $\vec{H}\|\vec{c}$, $\angle\vec{H}\vec{y} = 32.5°$ and $\angle\vec{H}\vec{z} = 57.5°$ apply. A comparison of the g_{eff} values calculated by using these angles with the experimental *g*

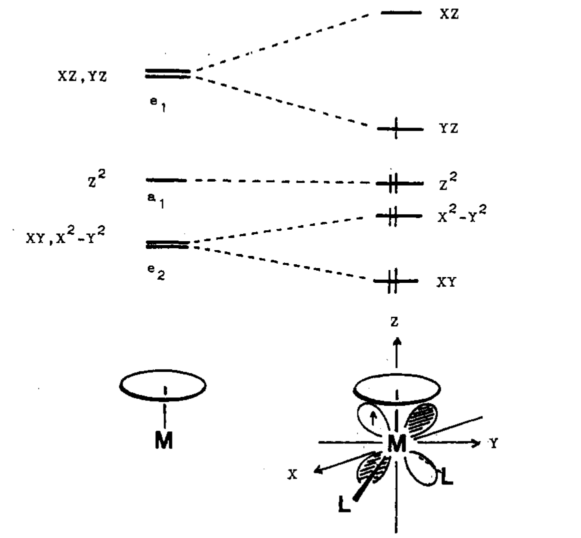

Figure 4. Crystal field splitting scheme for a half-sandwich moiety ($C_{\infty v}$) and for complexes of the type (η^6-arene)ML$_2$ (C_{2v}). The electron configuration shown refers to Co^{2+} (d^7).

factors for the two orientations $\vec{H}\|\vec{a}$ and $\vec{H}\|\vec{c}$ then allows the unequivocal assignment $g_y = 2.058$ and $g_z = 1.989$.

A derivation of the electronic ground-state configuration for (tol)Co(C_6F_5)$_2$, based on the assigned **g** tensor, will first be attempted by means of a simple crystal field splitting argument. Addition of two ligands to the half-sandwich unit (η^6-Ar)M will raise the degeneracy of the e_2 and e_1 sets and is expected to lead to the d-orbital sequence xy (a_2) < $x^2 - y^2$ (a_1) < z^2 (a_1) < yz (b_1) < xz (b_2) for the species (η^6-Ar)ML$_2$ as depicted in Figure 4. This orbital sequence, as well as the resultant single occupancy of a d_{yz} (b_1) orbital for the low-spin (d^7) complex (tol)Co(C_6F_5)$_2$, is in accord with the principal values of the **g** tensor determined in the present investigation. In C_{2v} symmetry,[9] mixing of the singly occupied orbital d_{yz} (b_1) with other filled or empty orbitals via spin–orbit coupling yields the following relations for the principal *g* values:[10]

$$g_x = 2.0023 + \frac{2\lambda}{\Delta E(d_{yz} - d_{x^2-y^2})} + \frac{6\lambda}{\Delta E(d_{yz} - d_{z^2})}$$

$$g_y = 2.0023 + \frac{2\lambda}{\Delta E(d_{yz} - d_{xy})}$$

$$g_z = 2.0023 - \frac{2\lambda}{\Delta E(d_{yz} - d_{xz})}$$

Although this simple approach neglects electron delocalization, it is in qualitative agreement with the experimental result $g_x > g_y > 2.0023 > g_z$ if the relative magnitudes of the energy gaps in the d-level scheme are considered. The nature of the HOMO as a b_1 orbital (metal component d_{yz}) was also inferred from extended Hückel calculations for model systems like (C_6H_6)NiH$_2$ and (C_6H_6)Fe(CO)$_2$.[5] Since the authors[5] state that the energy and composition of the HOMO b_1 depend on the electronic nature of the groups, we have performed an EHT–SCCC calculation for (tol)Co(C_6F_5)$_2$ itself.[11] In the frontier orbital region the following

(9) The exact point group symmetry, including the methyl group, is C_s (σ_{yz}).

(10) Goodman, B. A.; Raynor, J. B. *Adv. Inorg. Chem. Radiochem.* **1970**, *13*, 185.

(11) Hoffman, R. *J. Chem. Phys.* **1963**, *39*, 1397. Hoffmann, R.; Lipscomb, W. N. *Ibid.* **1962**, *36*, 3179, 3489; **1962**, *37*, 2872. The calculation was based on the geometry of (tol)Co(C_6F_5)$_2$ as described in ref 4. The values for H_{ii}(eV) were set equal to the VOIP's of the atoms:[12,13] H(1s), −13.6; C(2s), −21.4; C(2p), −11.4; F(2s), −40.1; F(2p), −21.0. The VOIP's for Co(eV) were determined by an iterative self-consistent charge and configuration procedure (SCCC):[13] Co(3d), −9.99; Co(4p), −8.33; Co(4s), −3.58. The resulting charge on Co (Mulliken population) is −0.015. The values for H_{ij} were calculated from H_{ii} and H_{jj} according to ref 14.

(12) Pritchard, H. O.; Skinner, H. A. *Chem. Rev.* **1955**, *55*, 745.

sequence was obtained:

MO	rel energy, cm^{-1}	Co(3d) component (coeff)
79	2379	xy (−0.962)
80	1660	z^2 (0.746), x^2-y^2 (−0.617)
81	1415	z^2 (0.648), x^2-y^2 (0.709)
82 (HOMO)	0	yz (0.979)
83 (LUMO)	−17695	xz (0.680)

The components $g_{x,y,z}$ of the **g** tensor, computed[15] by means of these relative state energies and by employing a spin–orbit coupling constant $\lambda(Co^{2+})$ of 533 cm^{-1} [16] while confirming the assignment of a $^2B_1$ ground state for (tol)Co$(C_6F_5)_2$, considerably differ in their magnitudes from the experimental values [calcd (λ = 533 cm^{-1}) g_x = 3.98, g_y = 1.94, g_z = 1.76]. Optimal agreement with experiment is achieved, if a greatly reduced effective spin–orbit coupling constant is used [calcd (λ = 100 cm^{-1}) g_x = 2.47, g_y = 2.05, g_z = 1.99; cf. Table I]. Whereas the effective value of λ may well be less than 50% of the free ion value when there is pronounced covalency in the ground state and the excited state coupled by the spin–orbit operator,[17–19] the reduction to 20%, required in the present case, appears somewhat large. Since larger energy differences ΔE and smaller Co coefficients would equally improve the agreement between theory and experiment, we contend that the inconsistency should be traced to inaccurate state energies and eigenfunctions as computed with the extended Hückel scheme. Rather than persuing this matter further here, we employ an effective λ of 100 cm^{-1} in the following discussion of the ^{59}Co hyperfine tensor. A detailed treatment of hyperfine splitting in (tol)Co$(C_6F_5)_2$ is hampered by the fact that $a_{iso}(^{59}Co)$ in fluid solution is unobservable, leading to uncertainty in the magnitudes and signs of the components $F_{x,y,z}$ of the traceless ^{59}Co hyperfine tensor **F**. Furthermore, the absence of resolved ligand hyperfine structure (^{1}H, ^{19}F) renders an independent estimate of the degree of covalency impossible. However, in order to choose between the eight possible combinations for the signs of $[A_x,A_y,A_z(^{59}Co)]_{exptl}$, recourse will be taken to the extended Hückel results. On the basis of the computed state energies, a calculation[20] of the principal values of the **F** tensor yields F_x = −57, F_y = +42, F_z = +15 (10^{-4} cm^{-1}) by using $P(Co^{2+})$ = 254 × 10^{-4} cm^{-1} and F_x = −45, F_y = +33, F_z = +12 (10^{-4} cm^{-1}) by using $P(Co^0)$ = 200 × 10^{-4} cm^{-1}. Agreement with experiment is best with the sign combination A_x = −38.2, A_y = +22.8, A_z = +12.0 (10^{-4} cm^{-1}), which leads to the experimental **F** tensor components F_x = −37.1, F_y = +23.9, F_z = +13.1 (10^{-4} cm^{-1}).

By way of summary it may be stated that from single-crystal EPR data a $^2B_1$ ground state[23] is unequivocally established for (tol)Co$(C_6F_5)_2$, the unpaired electron occupying an orbital of predominantly d_{yz} character. In order to achieve good numerical agreement between the experimental data and the **g** tensor calculated on the basis of extended Hückel results, covalency has to be accounted for by drastically reducing the spin–orbit coupling constant of the central metal. It is gratifying, though, that the same reduction factor also leads to a calculated ^{59}Co dipolar coupling tensor, which is in reasonable concordance with experiment.

Acknowledgment. This work was carried out during a term of sabbatical leave C.E. spent at Zürich University. Support by the Swiss National Foundation for Scientific Research (Project 2.442-0.82) is gratefully acknowledged. We also thank Dr. E. Dubler for his help with some crystallographic work.

Registry No. (η^6-tol)Co(η^1-C_6F_5)$_2$, 60528-58-7.

Supplementary Material Available: Background and details of the calculations of the elements of the **g** and **A** tensors (15 pages). Ordering information is given on any current masthead page.

(13) Basch, H.; Viste, A.; Gray, H. B. *Theor. Chim. Acta* **1965**, *3*, 458.
(14) Ammeter, J. H.; Bürgi, H.-B.; Thibeault, J. C.; Hoffmann, R. *J. Am. Chem. Soc.* **1978**, *100*, 3686.
(15) The details of the calculation are available as supplementary material.
(16) Griffith, J. S. "The Theory of Transition Metal Ions"; Cambridge University Press: New York, 1961.
(17) Atherton, N. M. "Electron Spin Resonance"; Ellis Horwood: Chichester, U.K., 1973.
(18) McGarvey, B. R. *Transition Met. Chem.* **1966**, *3*, 89–201.
(19) McGarvey, B. R. *Can. J. Chem.* **1975**, *53*, 2498. Malatesta, V.; McGarvey, B. R. *Ibid.* **1975**, *53*, 3791.
(20) Excited doublet states only were considered, and the values λ = 100 cm^{-1}, $P = g_e\beta_e g_N\beta_N\langle r^{-3}\rangle$ = 254 × 10^{-4} cm^{-1} (Co^{2+}), and P = 200 × 10^{-4} cm^{-1} (Co^0),[10] respectively, were employed. Judging from the extended Hückel results, a reduction of P from the value for Co^{2+} is called for since the central metal charge calculated in (tol)Co$(C_6F_5)_2$ is considerably smaller than +2 (vide supra). Details of the calculation are available as supplementary material.
(21) Daul, C.; Schläpfer, C. W.; Mohos, B.; Ammeter, J. H.; Gamp, E. *Comput. Phys. Commun.* **1981**, *21*, 385.
(22) Additional lines in the g_2 range of the X-band spectrum may be due to forbidden transitions ($\Delta m_I \neq 0$). In the simulation nuclear Zeeman and quadrupole effects were neglected. An anisotropic line width (with the same angular dependence as the g values) was assumed.
(23) In C_{2v} notation. In C_s notation, (σ_{yz}) is $^2A'$.